Impact of pH on the stability, dissolution and aggregation kinetics of Silver Nanoparticles

Ishara Fernando [a,b], Yan Zhou [b,c *]

[a]Interdisciplinary Graduate School, Nanyang Technological University, Singapore 639798.

[b]Advanced Environmental Biotechnology Centre, Nanyang Environment & Water Research Institute, Nanyang Technological University, 1 Cleantech Loop, CleanTech One, Singapore 637141.

[c]School of Civil & Environmental Engineering, Nanyang Technological University, 50, Nanyang Avenue, Singapore 639798.

*Corresponding author: Yan Zhou. E-mail: zhouyan@ntu.edu.sg

Abstract

Widespread usage of silver nanoparticles (AgNPs) in consumer products has resulted in their presence in the aquatic environment. The evolution of the properties of AgNPs with changes in pH and time in terms of colloidal stability, dissolution and aggregation were investigated in a series of short and long-term experiments using freshly synthesized uncoated AgNPs. The solution pH modifies the surface charge and the oxidative dissolution of AgNPs. As a result, the particle behavior varied in acidic and alkaline conditions. The particle size decreased with the increasing pH at a given time frame resulting in lower aggregation in the higher pH regime and increased particle stability. These results have been further proved with the direct

evidence obtained using time resolved in situ imaging acquired through Liquid cell transmission electron microscopy (LCTEM). Furthermore, the magnitude of the impact of the pH on the particle properties is higher than the impact of the dissolved oxygen concentration. The derived empirical formulae reflect that the AgNP oxidation depends on both dissolved oxygen and protons while the AgNP dissolution increasing with the increase of either of these. Overall, our results highlight the impact of the solution pH on the evolution of the properties of AgNPs over the time and provide an insight to confidently extend the results to predict the environmental transformation of AgNPs from ideal systems to the real.

Keywords: AgNPs, aggregation, pH, dissolution, particle stability, Liquid cell TEM

1. Introduction

The release of the silver nanoparticles (AgNPs) in to the aquatic environment can pose a potential risk to humans and other organisms (Ratte, 1999), when their levels surpass the safe permissible levels. The toxicity of AgNPs is related with the physical and chemical properties of the AgNPs.. These properties are further affected by the transformations such as dissolution, aggregation, redox reactions, flocculation, precipitation, sulfidation and the reactions with dissolved organic matter (Hotze et al., 2010; Levard et al., 2012; Dale et al., 2015). Above transformations may determine the fate, transport and the bioavailability of the AgNPs.

The environmental conditions where nano silver is suspended play a key role in governing the transformations of the AgNPs (Prathna et al., 2011). The factors affecting the environmental chemical conditions include pH (Axson et al., 2015), ionic strength (Badawy et al., 2010), dissolved oxygen, dissolved organic matter (Gunsolus et al., 2015) and microbial extracellular polymeric substances (EPS) (Kang et al., 2014). Of which, pH is one of the most important parameters governing the physical and chemical status (Hotze et al., 2010). Altering the liquid pH can influence the surface charge and the extent of dissolution of AgNPs, which eventually determines the fate of the AgNPs (Badawy et al., 2010).

Although there has been extensive research on the fate of AgNPs in the aquatic environment, the emphasis on the impact of pH on the aggregation and dissolution of AgNPs in environmentally relevant conditions is minimal. When the pH is considered, the environmental conditions usually observed are pH 5-8. Several studies focused on how extreme low pH would change the properties of AgNPs or how pH change would affect AgNPs in short term incubation conditions (Badawy et al., 2010; Elzey and Grassian, 2010; Stebounova et al., 2011; Peretyazhko et al., 2014; Tai et al., 2014; Axson et al., 2015). The pH range of 5-8 has not been vividly

investigated. Further, in most cases, the AgNPs used in the studies are commercially available particles or particles with different types of surface coatings. It should be noted that the coatings are likely detached from the surface once exposed to open environment (Li et al., 2013). Such detachment may also affect the true changes occurred.

In the highly acidic environment, the physical and chemical properties of the AgNPs can be modified and can affect their final form, fate and transformation in the environment (Levard et al., 2012). When exposed to environment, AgNPs may undergo different changes in their state, surface charge and morphology. Since the major transformation of AgNPs was observed to occur within several minutes of exposure to acid (Mwilu et al., 2013), the modifications have not been fully understood resulting in a lack of knowledge on these processes. For example, in the highly acidic environment, different degrees of particle growth have been observed in which the transformation proposed to occur via a step by step process: first via aggregation from the loss of coating followed by the release of ionic silver and finally the formation of precipitates such as silver chloride (Mwilu et al., 2013). An initial time point of measurement was normally after 10 mins in most of the previous studies, implying that there is a deficiency of data within a key time frame during which particles undergo their most rapid transformation (Peretyazhko et al., 2014; Tai et al., 2014), making the use of previous data challenging in interpretation of these phenomena.

This study provides an improved interpretation on how the solution pH altered the properties of particles over the time, due to its impact on the particle size and dissolved silver concentration. It can be further influenced by the dissolved oxygen as well according to the derived empirical formulae. In summary, the results provide an insight into how the particle

properties of AgNPs change as they age in the aquatic matrices and suggest how the particles evolve in the acidic and alkaline pH conditions.

2. Materials and methods

2.1 Synthesis of AgNPs

The silver nanoparticles used in the experiment were synthesized through an oxidation reduction method using silver nitrate and sodium borohydride. Detailed procedure on the synthesis with mechanism is mentioned in Fig. S1. High ionic strength in the liquid phase will cause aggregation (Li et al., 2011; Kazim et al., 2016) during AgNP synthesis, which can lead to failure in the synthesis of AgNPs (Mulfinger et al., 2007). Therefore, low initial $AgNO_3$ and $NaBH_4$ concentration is essential to reduce the solution ionic strength. Increasing the $NaBH_4/AgNO_3$ concentration ratio will enable more BH_4^- to be available in the solution hence stabilize uncoated AgNPs (Van Hyning and Zukoski, 1998). Three batches of AgNPs were prepared to evaluate the reproducibility and the results show production method was highly reliable (Fig. S2).

2.2 Stability of AgNPs under different pH

A series of samples was prepared from the pure AgNP stock solution to evaluate the changes over a period of 24 days. pH was varied in the range of 4-9 in the short-term experiments (up to 1 hour) and 5-8 in the long-term (0-24 days) experiments. Aliquots of 10% (w/v%) HNO_3 or 10% (w/v%) NaOH were used to adjust the pH value to the desired target. All the experiments were carried out in the ambient environment at 25 ± 2 $^{\circ}$C and analyzed in 2 min, 10 min, 20 min and 1 hour for short term experiments and in 1 hour, 24 hours, 7 days and 24 days for long term experiments. Before measurement, the samples were thoroughly mixed for approximately 1 min in screw capped 50 ml centrifuge tubes kept at room temperature (25± 2 $^{\circ}$C). Each type of

experimental sample was prepared in triplicate; therefore, the result represents the average of these three samples.

2.3 AgNP Characterization

UV-vis Spectrometry (Shimadzu UV- 4201 PC UV vis spectro-photometer, UK) was used to measure the localized surface plasmon resonance (SPR) of the AgNPs over the wavelength in the range of 300 – 800 nm. The particle size distribution of the AgNPs was measured by Dynamic Light Scattering (DLS) using a Zetasizer Nano (Malvern Instruments, UK) with a 1 cm optical cell. Each measurement was averaged over 10 runs of 2-3 mins each on which the Dispersion Technology Software V4.20 (Malvern Instruments Ltd.) was utilized to fit both single and multiple exponential algorithms to each autocorrelation function (Carpenter, 1977). Zeta potential of the experimental samples at different pH was measured with Zetasizer Nano at 25 ± 2 $^{\circ}$C.

The total silver concentration of the synthesized AgNP stock solution was measured by the acid digestion method. Briefly, 0.5 ml of 70% nitric acid with 0.5 ml of AgNP stock solution was incubated at 60 $^{\circ}$C for 12 hours. The digested solution was then diluted with DI water to a known volume with 1% (w/v%) HNO_3 solution. The dissolved Ag+ was quantified by an inductively coupled plasma optical emission spectrometer (ICP-OES, Perkin Elmer Instruments).

The dissolved Ag+ in the synthesized AgNPs and the experimental samples was quantified after removing the suspending AgNPs and the method used is described in SI.

Morphology, size and the energy dispersive x-ray spectroscopy (EDX) analysis of the AgNPs was observed using transmission electron microscopy (TEM) without solely relying on the hydrodynamic behaviour. Details on TEM sample preparation (Mehrabi et al., 2017) and imaging is mentioned in SI.

Liquid cell TEM (LCTEM) experiments were carried out using a Poseidon 210 liquid fluid holder (Protochips Inc.) with liquid cell e-chips containing silicon nitride windows of thickness of 50 nm. LCTEM investigation was performed using a JEOL 2010 HR TEM operated at 200 kV. All the in-situ images presented in this study were recorded in parallel beam TEM mode. Time-lapse TEM imaging was carried out with a dwell time of 0.2 s per frame and hundreds of frames at least for each sequence (Liu et al., 2016). For each experiment, freshly synthesized AgNPs was used with 10 % (w/v%) HNO_3 acid to investigate the aggregation phenomena in the acidic condition (pH ~ 5.5) and the DI water to investigate the aggregation phenomena in the neutral conditions.

Dissolution of the AgNPs induced by the irradiation of the electron beam in the DI water can be observed in some cases. However, recrystallization of dissolved ions was not observed under the conditions used in this study. This dissolution of AgNPs under these conditions depends on many factors such as dose rate, irradiation time and strength. It is beyond the scope of this study and will be separately discussed in a subsequent study. All the static images presented in this paper were acquired under the conditions when no obvious dissolution was observed.

2.4 Stability of AgNPs under different oxygen concentrations

It should be noted that dissolved oxygen (DO) level is a parameter that cannot be ignored when investigating the pH effect. To evaluate the stability of the synthesized AgNPs under different DO levels, three samples were prepared. The first sample was exposed to the ambient environment where there would be atmospheric oxygen exchange with the sample. The second sample was sparged with N_2 and capped immediately after N_2 sparging, and the capped sample was kept at the ambient environment. There would be some oxygen dissolved when the cap was

opened for sampling. The third sample was sparged with N_2, capped and kept in the anaerobic chamber. All the samples were covered with aluminium foil to avoid the impact of light on the AgNPs. The SPR peak, pH, zeta potential and the particle size of the three samples were monitored for two weeks and the results are mentioned in Fig. S10-12.

3. Results

3.1 Characterization of the synthesized AgNPs

The average size of the synthesized AgNPs was 26 ± 1.248 nm. TEM results show the diameters of more than 81% of the counted AgNPs ranged between 10-50 nm. The particles were reasonably monodispersed in the suspension and had a spherical shape (Fig. S4(a)) with a light-yellow color in the solution (Fig. S4(b)). The size value obtained using DLS was the peak size based on the intensity distribution (36.76 ± 5.172 nm) (Fig. S4(c)). The synthesized nanoparticles showed a characteristic peak at the wavelength of 391 ± 2 nm in the UV-Vis absorption spectrum with a peak-absorbance of 0.726 (Fig. S4(d)). The total silver concentration of the synthesized AgNPs was 5.929 ± 0.025 mg/L with a dissolved silver concentration of 2.278 ± 0.004 mg/L. The pH and the zeta potential of the pure AgNP stock solution was reported to be 8.03 and -29 ± 1.9 mV respectively.

3.2 Short-term pH impact

The peak absorbance at the characteristic wavelength (391 ± 2 nm for AgNPs) implies the concentration of AgNPs in the solution (Mulvaney, 1996). The freshly synthesized AgNPs (also denoted as pure AgNPs) displayed a clean and relatively narrow SPR with a peak absorbance of 0.701 at 391 nm (Fig. 1). The introduction of acid lowered the SPR peak to 0.15 and 0.35 at pH 5 and 6 respectively (Fig. 1(a) & (b)). In the condition of pH 7, where no acid or base was added and only diluted with DI water, the SPR was reduced from original 0.701 to 0.342 due to the

dilution hence causing hindrance to the solution matrix of pure AgNPs (Fig. 1(c)). At pH 8 (minor pH adjustment from pure AgNPs solution), the SPR reduced from 0.701 to 0.61 after 2 minutes and remained almost stable for the rest 1 hour of evaluation (Fig. 1(d)).

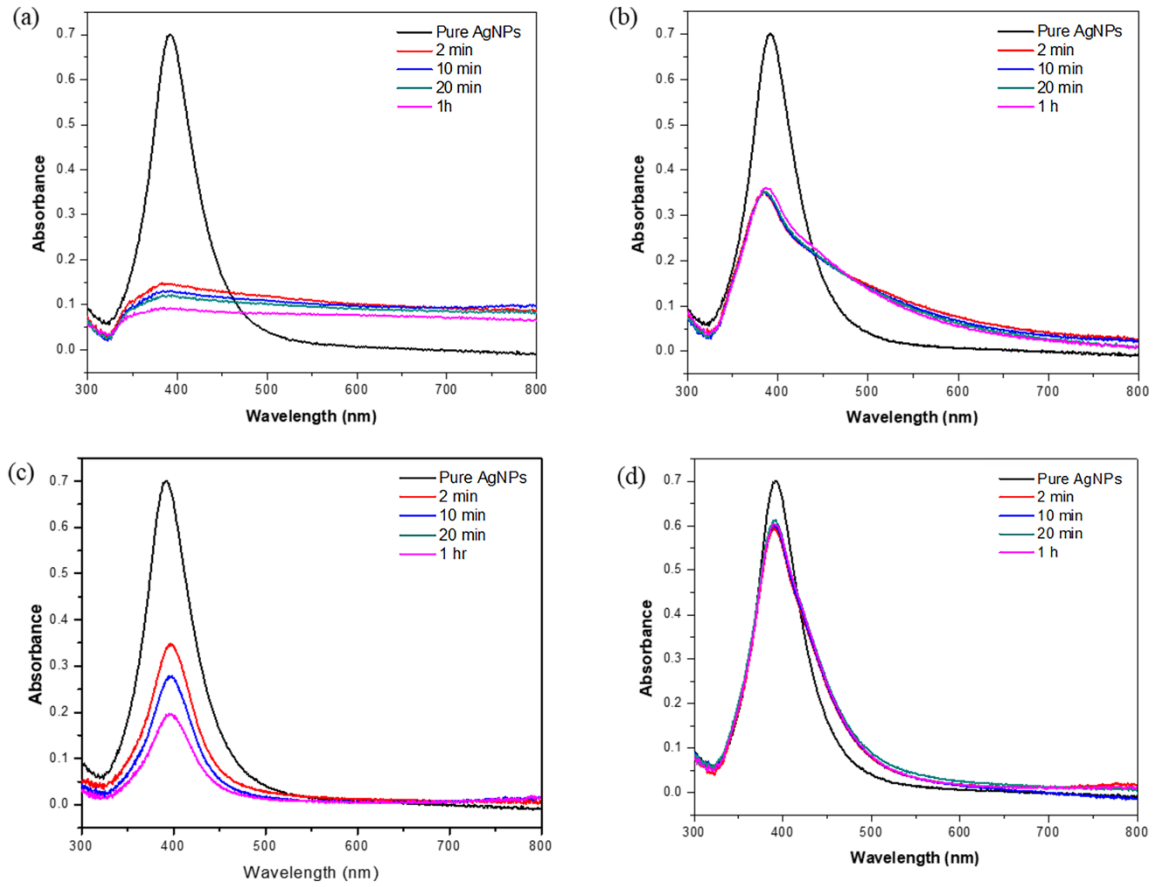

Fig. 1. Short-term changes in the UV vis spectrum at (a) pH 5 (b) pH 6 (c) pH 7 and (d) pH 8

Rapid size change in the AgNPs was observed in the first few minutes (Fig. 2(a)). From a z average size of 36.76 nm (mode 38.32 nm), the particle size increased to a z average (z avg) size of 433.2 nm within 1 hour, when the solution pH was changed to pH 4. Similarly, the rate of change of z avg diameter was also changed within this 1-hour time (Table S2). The largest size was observed at pH 4, and the size gradually decreased with the increasing pH.

The size values obtained at different pH were further confirmed by the results obtained from UV vis spectrum (Fig. 2(b)) and the particle size distribution (Fig. 2(c)). The UV vis spectrum shows a significant decrease in the absorbance from 0.701 to 0.19 at pH 7 within 1 hr. The peak absorbance further decreased with the decreasing pH (Fig. 2(b)), meantime, a considerable peak absorbance was visible at the wavelength from 500 - 600 nm. It has been reported that 500 - 600 nm is the wavelength used for characterization of AgNP aggregates(Paramelle et al., 2014). Thus, significant amount of AgNP aggregates may appear under low pH conditions. For the solution with the pH in the alkaline region, the decrease in the absorbance was far less compared to the acidic region suggesting that the solution was more stabilized in the alkaline pH. When pH was above 8, the peak absorbance wavelength shifted slightly to the right (Fig. 2(b)), while maintaining the peak absorbance almost at a constant level regardless of the pH value. The particle size distribution at acidic pH shifted to the right with the peaks in between 300-400 nm (Fig. 2(c)) suggesting that the particles were destabilized in the acidic conditions and larger sized particles were formed due to the increased particle aggregation (Prathna et al., 2011). In contrast, the particles in the alkaline conditions became more stable with a particle size distribution similar as pure AgNPs (Fig. 2(c), Table S1). The dissolved silver concentration shows a decreasing trend with the increasing pH (Fig. 2(d)).

Above observation provides evidence that the short-term aggregation kinetics of the AgNPs is dependent on the solution pH. A higher rate of change was observed in the lower pH at pH 4 (Table S2). With the increasing pH, the rate of change decreased depicting that the rate of aggregation was higher in the acidic region compared to alkaline region (Table S2). The phenomenon of aggregation could be divided into two main phases (Hotze et al., 2010). The first phase was where the faster rate of aggregation occurs, which corresponded to the aggregation of

individual AgNPs into smaller clusters. During the second phase these smaller clusters came together to form larger clusters which happened in a lower rate. As shown in Fig. 2(a), this phenomenon took place in the acidic region whereas in the alkaline region or in higher pH, particle size remained almost constant during the experimental period of 1 hour.

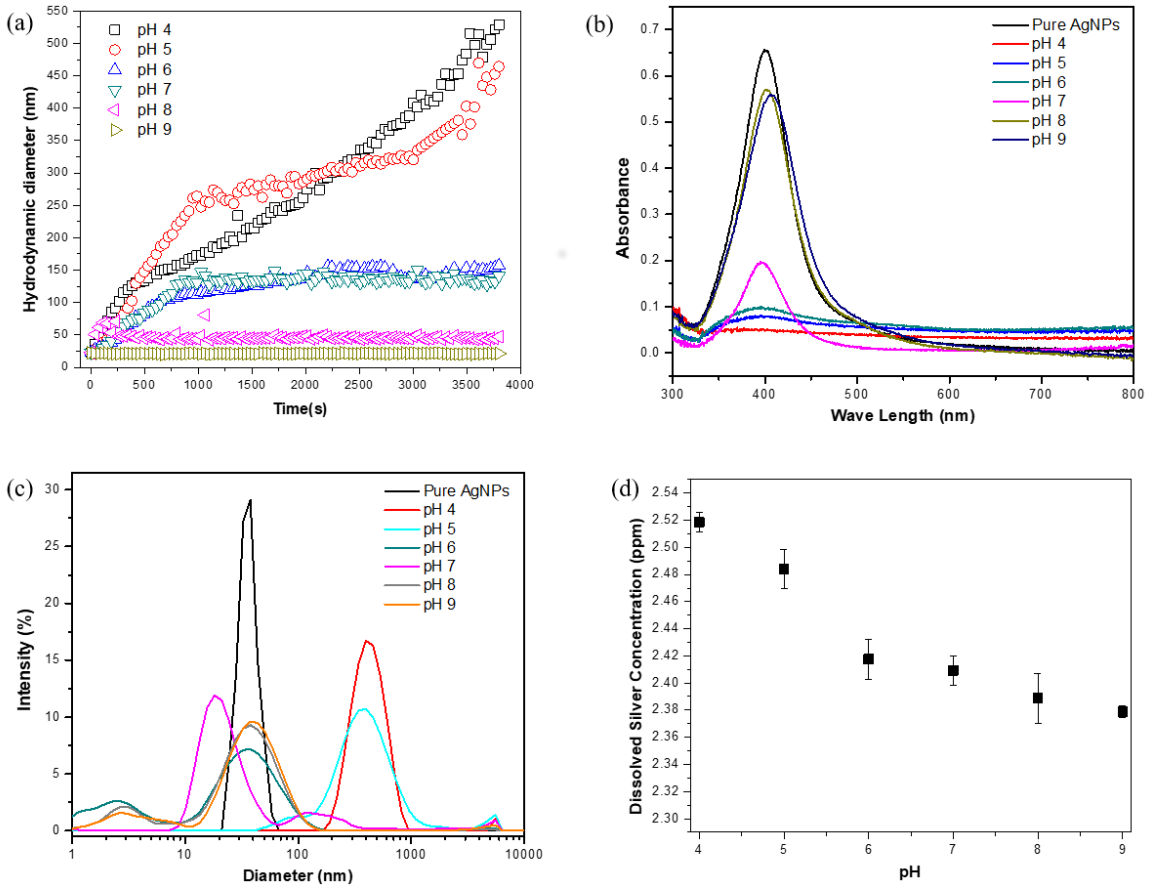

Fig. 2. Change in the (a) aggregation kinetics (b) UV vis spectrum (c) particle size distribution and (d) dissolved silver concentration during 1 hour

3.3 Long-term pH impact

pH 5, 6, 7 and 8 were chosen for the long-term study. The results show that the SPR peak decreased with the time for all pH conditions with significant changes occurred at pH 5, 6 and 7

(Fig. 3(a), (b) and (c)) and the highest rate of change occurred in pH 5. At pH 8, there was a red shift in the peak absorbance but the SPR shifted back slightly at the later stage and remained above 0.6 (Fig. 3(d)).

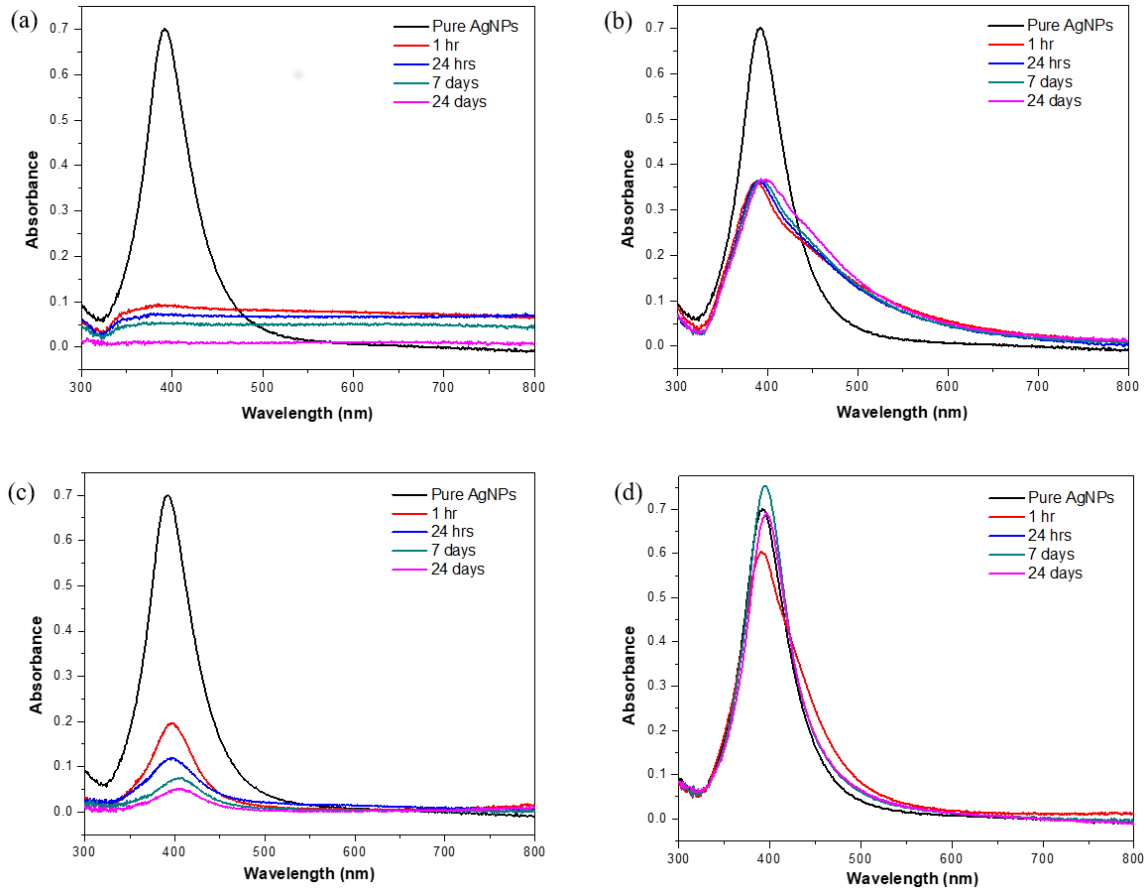

Fig. 3. Change in the UV vis spectrum at (a) pH 5 (b) pH 6 (c) pH 7 and (d) pH 8

The particle size distribution in the acidic condition (Fig. 4(a)) shows that most of the particles were larger (peak at 342 nm) than in the pure AgNPs after the first hour. TEM imaging (Fig. S5) displays the AgNPs in aggregated clusters which could be attributed to the solution destabilization and subsequent aggregation. The results indicate that the aggregation took place within the first hour in a faster rate, then remained relatively stable after 24 hours. Over the

extended period, more particles evolved into larger particles. This peak then remained largely unchanged although there was some increase in a small number of much larger aggregates at approximately 4000 nm. In the neutral and alkaline pH conditions, the particle size remained below 100 nm throughout the experimental period (Fig. 4(c) & (d)). TEM images obtained for pH 8 depict more stabilized individual particles compared to the images obtained at the acidic conditions (Fig. S5).

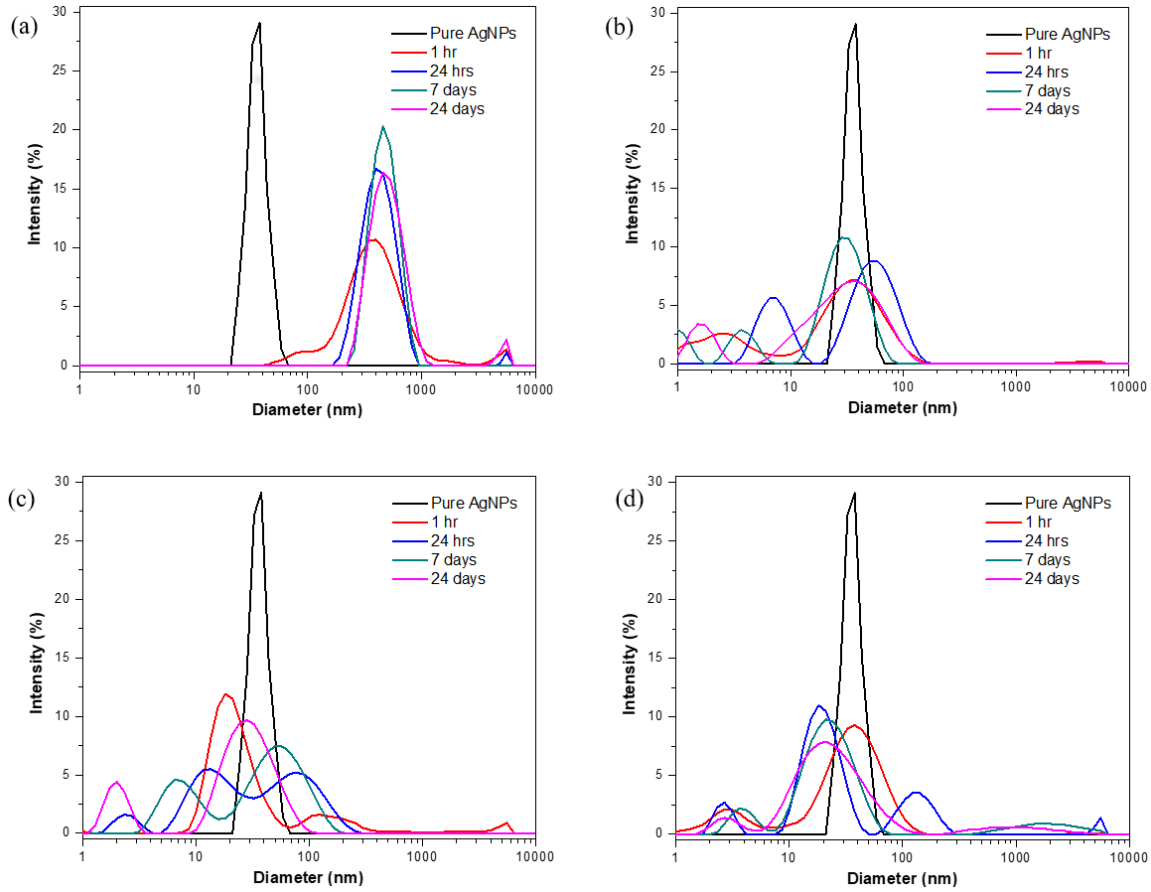

Fig. 4. Change in the particle size distribution at (a) pH 5 (b) pH 6 (c) pH 7 and (d) pH 8

The zeta potential results obtained for solutions at different pH after 24 hours incubation can be found in Fig. S6. The results support the results obtained using DLS and UV vis and show

that during the alkaline conditions the particles were relatively stable than in the acidic conditions due to the re-stabilization occurred by the negatively charged hydroxyl ions resulting in negative zeta potential. The positive yet the less than 25 mV zeta potential value obtained at pH 5, shows the degree of de-stability occurred in the acidic conditions, due to the addition of protons into the solution which hindered the stability of negatively charged AgNPs in the solution.

The increase in the dissolved silver concentration at pH 5 and 6 (Fig. S7(a) & (b)) was probably due to the ionic silver released from AgNPs or due to the oxidative dissolution of AgNPs (Peretyazhko et al., 2014). On the other hand, Ag+ concentration at pH 7 and 8 decreased with the time (Fig. S7(c) & (d)). The degree of the dissolution of ionic silver from AgNPs reduced with the increasing pH (Table S2). To verify the potential precipitation, EDX analysis of the samples were carried out and the results are mentioned in Fig. S8 & Table S3. The EDX results reveal that there was no precipitation observed in pH 5, 6 and 8.

3.4 In-situ imaging of AgNP aggregation

The aggregation of AgNPs under acidic and neutral conditions was observed using in-situ TEM imaging. The time series TEM images were processed and illustrated in the Fig. 5. Original images can be found in Fig. S9. In the acidic conditions, all the particles present within the frame aggregated within 85.8s (Fig. 5 - upper row). On the other hand, there were individual particles in the frame without attaching to the aggregates that previously formed after 175s in the neutral condition (Fig. 5 - lower row). According to these time series images it is further evident that the rate of aggregation is higher in the acidic conditions compared to the neutral conditions.

In the Fig. 5, the aggregates formed in each frame were circled in red. According to the time series images, the time taken for two single particles to aggregate was 34.6 s and 64.5 s

under acidic and natural conditions, respectively. However, the time required for a single particle to aggregate into an already formed aggregate was shorter (22.6 s and 24.9 s under acidic and natural conditions, respectively). This implies the energy barrier that the single particles need to overcome may be higher compared to the same for a cluster or an aggregate(Chen et al., 2015). This can be clearly viewed in the videos showing the movement of particles in neutral and acidic solution (SI Movie 1 & 2).

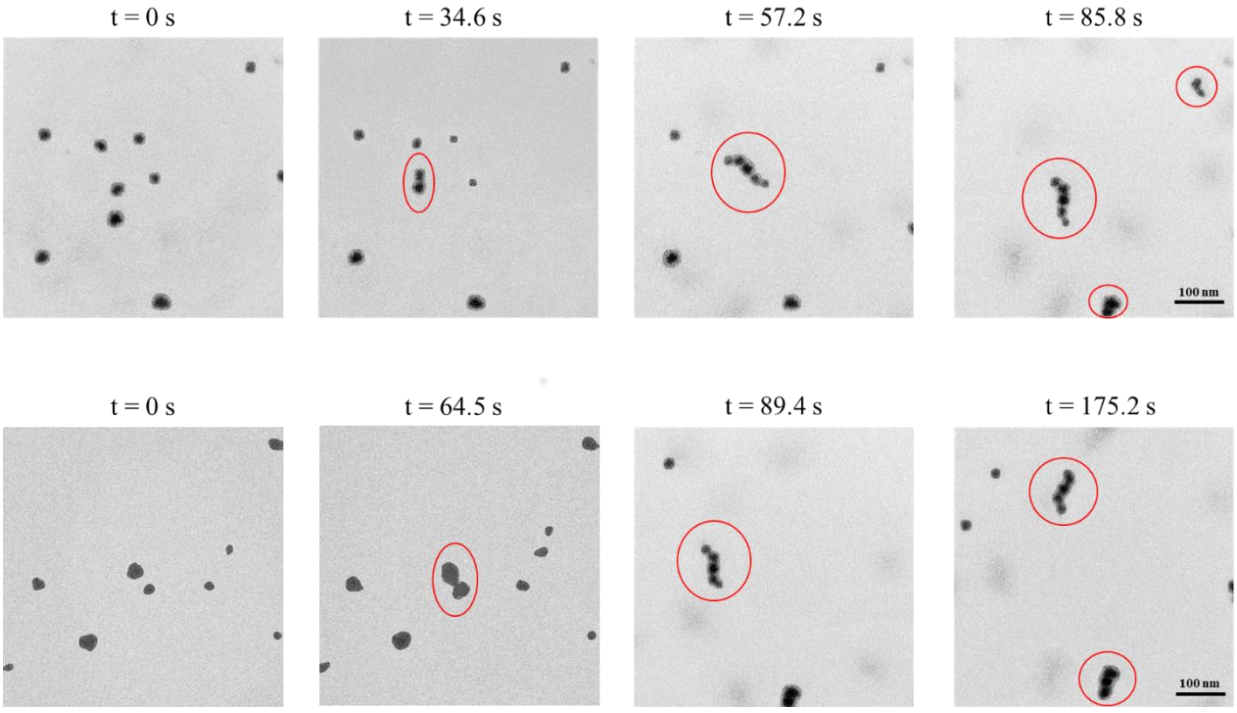

Fig. 5. Formation of AgNPs aggregates in the time series in acidic condition (upper row) and neutral condition (lower row)

4. Discussion

The aging process of the spherical, freshly synthesized uncoated AgNPs during the short term experiments took place at a higher rate of reaction compared to the same during the long

term experiments (Table S2), while aggregation dominated the short term transformations. Understanding the impact of the pH will not be completed without studying the potential impact of the DO in the solution matrix. Therefore, the DO effect has also been discussed in terms of aggregation and dissolution during this study (Fig. S10-12). However, the results reveal that the impact of DO during the short-term experiments was negligible compared to the impact during the long-term study. The individual and the cumulative impact of DO and pH on the oxidative dissolution and aggregation are discussed in detail in this section.

In this study, it was assumed that the dissolved oxygen level in all the samples remained constant (saturated level) and the impact from DO was minor compared to that from pH. To verify the hypothesis, the stability of pure AgNPs without pH adjustment was monitored over 15 days (Fig. S10(a)). The SPR peak change of the pure AgNPs was used as a baseline to illustrate the DO (sole factor) impact on AgNPs (Fig. S13). The SPR curves obtained from various pH were normalized with the peak absorbance of pure AgNPs on respective days (e.g. day 1). This is to eliminate the changes caused by background DO and reflect the true effect of pH. A set of the normalized curves obtained on day 1 are shown in the Fig. S14. The results confirmed that the change in the SPR caused by pH was evidently significant compared to the change caused by DO. This information clearly depicts that the impact of pH on the aggregation hence the colloidal stability of AgNPs was higher compared to the impact of DO.

The oxidative dissolution of AgNPs in the solution takes place with the reactions where the metallic Ag is oxidized by oxygen and subsequently reacts with protons (Equation (1), (2)) (Peretyazhko et al., 2014; Zhou et al., 2016) .

$$4Ag_{(s)} + O_2 \rightarrow 2Ag_2O_{(s)} \quad (1)$$

$$Ag_2O_{(s)} + 2H^+ \rightarrow 2Ag^+ + H_2O \quad (2)$$

As illustrated in the Equation (1) the oxygen concentration plays a critical role in the dissolution of AgNPs. During the experiments, it was assumed that the oxygen concentration was kept constant, since DI water was used from the same source and all the experiments were conducted in the ambient environment. The overall reaction took place in the solution can be illustrated as in Equation (3). It shows that the DO and solution pH directly contribute to the dissolved silver concentration.

$$4Ag_{(s)} + O_2 + 4H^+ \rightarrow 4Ag^+ + 2H_2O \quad (3)$$

The hard sphere collision theory can be utilized to determine the dissolution kinetics of AgNPs (Zhang et al., 2011). According to the theory, rate (γ_{Ag^+}) of ionic silver (Ag^+) release during the overall oxidation of $Ag_{(s)}$ to Ag^+ from the above reaction is shown in the Equation (4).

$$\gamma_{Ag^+} = \frac{3}{4}\left(\frac{8\pi k_B T}{m_B}\right)^{1/2} \rho^{-1} exp\left(\frac{-E_a}{k_B T}\right) r^{-1}[O_2]^{0.5}[H^+]^2[Ag] \quad (4)$$

where k_B is the Boltzmann constant; T is the absolute temperature (K); m_B is the molecular weight of the reactant B (g/mol), which is either oxygen or protons in this case; ρ is the density of the AgNPs (g/cm^3); E_a is the activation energy (J); r is the particle radius (nm); $[O_2]$ and $[H^+]$ are the molar concentrations (mol/L) of dissolved oxygen and hydrogen ions; and $[Ag]$ is the mass concentration of silver in the system (g/L).

At a fixed time, temperature (25 ± 2 °C), DO, $[Ag]$, the original particle size of the samples, m_B and r can be considered as constants. If the results were to be compared across with different pH, Equation (4) can be rearranged with the following expression:

$$\gamma_{Ag^+} = k[H^+]^2 \quad (5)$$

with

$$k = \frac{3}{4}\left(\frac{8\pi k_B T}{m_B}\right)^{1/2} \rho^{-1} exp\left(\frac{-E_a}{k_B T}\right) r^{-1}[O_2]^{0.5}[Ag] \quad (6)$$

According to the Equation (5), the rate of dissolution of AgNPs is proportional to the $[H^+]^2$. This indicates that a minor increase in the H^+ concentration can result in a higher rate of dissolution. This is evident from the results obtained, which shows that with the decreasing pH, the dissolved silver concentration increased in a higher rate (Table S2), compared to the higher pH. These observations are in consistence with the previous results (Kittler et al., 2010; Zhang et al., 2011; Peretyazhko et al., 2014) and demonstrate that the rate of dissolution will increase with the decreasing pH. The complete dissolution of the AgNPs will occur only when the pH is further lowered or at a longer exposure period.

Based on the SPR peak obtained for the pure AgNPs (Fig. S4(d)), it can be confirmed that the initial surface of the AgNPs was free of an oxide layer. With the exposure to different pH, the oxide layer of the AgNPs has been changed. According to the EDX results, an increasing trend in the oxygen concentration with the decreasing pH has been observed (Table S3). It is possible that the low pH and high DO induced the formation of an oxide layer during the incubation. Therefore, it is confirmed that dissolution of AgNPs was pH dependent, which is related to the dissolution of this silver oxide (Ag_2O) layer (Equation (2)). The dissolution of the oxide layer may expose metallic silver, which also exhibits pH dependent dissolution (Equation (3)) (Zhang et al., 2011).

The decrease in SPR normally reflects the change in particle size or morphology (Zou et al., 2015). This study reveals that the particle morphology remained spherical regardless of aggregation (Fig. S5), while only particle size changed. Further, the AgNP concentration at the lower pH was reduced, reflecting a reduction in the stability of the particles. Both particle size and dissolved silver increased under lower pH. The results obtained on the impact of pH on the

aggregation and dissolution of AgNPs, were consistent with the previous work (Liu and Hurt, 2010; Yu et al., 2013; Peretyazhko et al., 2014).

Aggregation of AgNPs takes place when the kinetic energy of the Brownian motion overcomes the energy barrier between the nanoparticles. The energy barrier would be reduced in acidic solution as the nanoparticles become essentially neutral (Badawy et al., 2010) due to the addition of positive charged protons to the negative charged AgNPs. Using in-situ TEM imaging, this study demonstrates that the rate of aggregation increased with the introduction of the protons. The process of aggregation took place with the introduction of protons to the AgNPs in the aquatic solution. The external protons introduced to the system deteriorated the electron cloud around the particles and attracted the electrons towards them, and eventually destabilized AgNPs (Hoek and Agarwal, 2006). However, in the alkaline conditions, the AgNPs were more stable in solution, since the hydroxyl ions with the negative charge strengthened the negative charges among the AgNPs, hence, the repulsion force increased among the particles. When the hydroxyl ions were introduced to the system of AgNPs in the aquatic solution, they were repelled by the negatively charged AgNPs. This in turn strengthened the electron cloud around the particles and restabilized the electron cloud which enhanced the stability of the particles in the solution. The mechanisms took place in acidic and alkaline conditions are graphically summarized in the Fig. S15(a) & (b).

During this study, we conducted a series of experiments to get a better understanding on how the properties of AgNPs change over time as a function of pH. This indicates a deviation from the previous research with AgNPs that were conducted under different conditions. Therefore, the outcome of this study provides an insight into the fate of the AgNPs. It will also

help to identify the conditions under which the studies conducted with freshly synthesized AgNPs can be confidentially extended to explain such behavior in the environment.

5. Conclusions

This study demonstrates the time resolved changes in the properties of uncoated AgNPs as they were exposed to different pH conditions in the aquatic environment. The particles were freshly synthesized and utilized in the study to allow the monitoring and understanding on the aging process of the particles. It was observed that pH had a strong influence on the properties of the AgNPs, as it governed the surface charge of AgNPs hence aggregation (Fig. 2) and oxidative dissolution (Fig. S7). It was found that AgNPs were dominantly affected by the pH under the phenomena of aggregation and dissolution. At acidic and neutral pH, the particles were destabilized resulting in higher rate of aggregation. In the alkaline conditions, the particles were re-stabilized due to the presence of hydroxyl ions resulting in more stable suspensions. The short-term results reveal that the impact of DO on the fate of the AgNPs is negligible compared to the effect of pH, and aggregation dominate the initial transformation. During the long-term study, the aging process of particles happens at a lower rate compared to the short term study but provide distinct trends in the particle properties in terms of oxidative dissolution and aggregation as a function of pH and DO. These results provide an insight to understand the influence of solution pH on the aging of negatively charged AgNPs, which is essential to evaluate the fate and transport of engineered as well as natural NPs and subsequently their impact on the environment.

Statement for competing interests

The authors declare no competing interests.

Acknowledgement

The authors would like to acknowledge the support received from the Central Environmental Science & Engineering Laboratory (CESEL) and Dr. Tay Yee Yan from the Facility for Analysis, Characterization, Testing & Simulation (FACTS).

References

Axson, J.L., Stark, D.I., Bondy, A.L., Capracotta, S.S., Maynard, A.D., Philbert, M.A., Bergin, I.L., Ault, A.P., 2015. Rapid Kinetics of Size and pH-Dependent Dissolution and Aggregation of Silver Nanoparticles in Simulated Gastric Fluid. Journal of Physical Chemistry C.

Badawy, A.M.E., Luxton, T.P., Silva, R.G., Scheckel, K.G., Suidan, M.T., Tolaymat, T.M., 2010. Impact of Environmental Conditions (pH, Ionic Strength, and Electrolyte Type) on the Surface Charge and Aggregation of Silver Nanoparticles Suspensions. Environmental Science & Technology 44, 1260-1266.

Carpenter, D.K., 1977. Dynamic Light Scattering with Applications to Chemistry, Biology, and Physics (Berne, Bruce J.; Pecora, Robert). Journal of Chemical Education 54, A430.

Chen, Q., Cho, H., Manthiram, K., Yoshida, M., Ye, X., Alivisatos, A.P., 2015. Interaction Potentials of Anisotropic Nanocrystals from the Trajectory Sampling of Particle Motion using in Situ Liquid Phase Transmission Electron Microscopy. ACS Central Science 1, 33-39.

Dale, A.L., Casman, E.A., Lowry, G.V., Lead, J.R., Viparelli, E., Baalousha, M., 2015. Modeling Nanomaterial Environmental Fate in Aquatic Systems. Environmental Science & Technology 49, 2587-2593.

Elzey, S., Grassian, V.H., 2010. Agglomeration, isolation and dissolution of commercially manufactured silver nanoparticles in aqueous environments. Journal of Nanoparticle Research.

Gunsolus, I.L., Mousavi, M.P.S., Hussein, K., Bühlmann, P., Haynes, C.L., 2015. Effects of Humic and Fulvic Acids on Silver Nanoparticle Stability, Dissolution, and Toxicity. Environmental Science & Technology 49, 8078-8086.

Hoek, E.M.V., Agarwal, G.K., 2006. Extended DLVO interactions between spherical particles and rough surfaces. Journal of Colloid and Interface Science 298, 50-58.

Hotze, E.M., Phenrat, T., Lowry, G.V., Mellon, C., 2010. Nanoparticle Aggregation : Challenges to Understanding Transport and Reactivity in the Environment. 1909-1924.

Kang, F., Alvarez, P.J., Zhu, D., 2014. Microbial extracellular polymeric substances reduce Ag+ to silver nanoparticles and antagonize bactericidal activity. Environmental science & technology 48, 316-322.

Kazim, S., Jäger, A., Steinhart, M., Pfleger, J., Vohlídal, J., Bondarev, D., Štěpánek, P., 2016. Morphology and Kinetics of Aggregation of Silver Nanoparticles Induced with Regioregular Cationic Polythiophene. Langmuir 32, 2-11.

Kittler, S., Greulich, C., Diendorf, J., Koller, M., Epple, M., 2010. Toxicity of silver nanoparticles increases during storage because of slow dissolution under release of silver ions. Chemistry of Materials 22, 4548-4554.

Levard, C., Hotze, E.M., Lowry, G.V., Brown Jr, G.E., 2012. Environmental transformations of silver nanoparticles: impact on stability and toxicity. Environmental science & technology 46, 6900-6914.

Li, X., Lenhart, J.J., Walker, H.W., 2011. Aggregation Kinetics and Dissolution of Coated Silver Nanoparticles.

425 Li, Y., Zhang, W., Niu, J., Chen, Y., 2013. Surface-Coating-Dependent Dissolution,
426 Aggregation, and Reactive Oxygen Species (ROS) Generation of Silver Nanoparticles under
427 Different Irradiation Conditions. Environmental Science & Technology 47, 10293-10301.
428 Liu, J., Hurt, R.H., 2010. Ion release kinetics and particle persistence in aqueous nano-silver
429 colloids. Environmental science & technology 44, 2169-2175.
430 Liu, J., Wang, Z., Sheng, A., Liu, F., Qin, F., Wang, Z.L., 2016. In Situ Observation of Hematite
431 Nanoparticle Aggregates Using Liquid Cell Transmission Electron Microscopy.
432 Mehrabi, K., Nowack, B., Arroyo Rojas Dasilva, Y., Mitrano, D.M., 2017. Improvements in
433 Nanoparticle Tracking Analysis To Measure Particle Aggregation and Mass Distribution: A Case
434 Study on Engineered Nanomaterial Stability in Incineration Landfill Leachates. Environmental
435 Science & Technology 51, 5611-5621.
436 Mulfinger, L., Solomon, S.D., Bahadory, M., Jeyarajasingam, A.V., Rutkowsky, S.A., Boritz, C.,
437 2007. Synthesis and Study of Silver Nanoparticles. Journal of Chemical Education 84, 322.
438 Mulvaney, P., 1996. Surface Plasmon Spectroscopy of Nanosized Metal Particles. Langmuir 12,
439 788-800.
440 Mwilu, S.K., El Badawy, A.M., Bradham, K., Nelson, C., Thomas, D., Scheckel, K.G.,
441 Tolaymat, T., Ma, L., Rogers, K.R., 2013. Changes in silver nanoparticles exposed to human
442 synthetic stomach fluid: Effects of particle size and surface chemistry. Science of The Total
443 Environment 447, 90-98.
444 Paramelle, D., Sadovoy, A., Gorelik, S., Free, P., Hobley, J., Fernig, D.G., 2014. A rapid method
445 to estimate the concentration of citrate capped silver nanoparticles from UV-visible light spectra.
446 Analyst 139, 4855-4861.

Peretyazhko, T.S., Zhang, Q.B., Colvin, V.L., 2014. Size-Controlled Dissolution of Silver Nanoparticles at Neutral and Acidic pH Conditions: Kinetics and Size Changes. Environmental Science & Technology 48, 11954-11961.

Prathna, T.C., Chandrasekaran, N., Mukherjee, A., 2011. Studies on aggregation behaviour of silver nanoparticles in aqueous matrices: Effect of surface functionalization and matrix composition. Colloids and surfaces.

Ratte, H.T., 1999. Bioaccumulation and toxicity of silver compounds: A review. Environmental Toxicology and Chemistry 18, 89-108.

Stebounova, L.V., Guio, E., Grassian, V.H., 2011. Silver nanoparticles in simulated biological media: a study of aggregation, sedimentation, and dissolution. Journal of Nanoparticle Research 13, 233-244.

Tai, J.T., Lai, C.S., Ho, H.C., Yeh, Y.S., Wang, H.F., Ho, R.M., Tsai, D.H., 2014. Protein Silver Nanoparticle Interactions to Colloidal Stability in Acidic Environments. Langmuir 30, 12755-12764.

Van Hyning, D.L., Zukoski, C.F., 1998. Formation Mechanisms and Aggregation Behavior of Borohydride Reduced Silver Particles. Langmuir 14, 7034-7046.

Yu, S.-j., Yin, Y.-g., Chao, J.-b., Shen, M.-h., Liu, J.-f., 2013. Highly dynamic PVP-coated silver nanoparticles in aquatic environments: chemical and morphology change induced by oxidation of Ag0 and reduction of Ag+. Environmental science & technology 48, 403-411.

Zhang, W., Yao, Y., Sullivan, N., Chen, Y., 2011. Modeling the primary size effects of citrate-coated silver nanoparticles on their ion release kinetics. Environmental science & technology 45, 4422-4428.

Zhou, W., Liu, Y.-L., Stallworth, A.M., Ye, C., Lenhart, J.J., 2016. Effects of pH, Electrolyte, Humic Acid, and Light Exposure on the Long-Term Fate of Silver Nanoparticles. Environmental Science & Technology 50, 12214-12224.

Zou, X., Shi, J., Zhang, H., 2015. Morphological evolution and reconstruction of silver nanoparticles in aquatic environments: the roles of natural organic matter and light irradiation. J Hazard Mater 292, 61-69.